Original article

GB7 acetate, a *galbulimima* alkaloid from *Galbulimima belgraveana*, possesses anticancer effects in colorectal cancer cells

Ziyin Li [a, 1], Lianzhi Mao [a, 1], Bin Yu [b], Huahuan Liu [a], Qiuyu Zhang [a], Zhongbo Bian [a], Xudong Zhang [a], Wenzhen Liao [a, *], Suxia Sun [a, **]

[a] *Department of Nutrition and Food Hygiene, Guangdong Provincial Key Laboratory of Tropical Disease Research, School of Public Health, Southern Medical University, Guangzhou, 510515, China*
[b] *School of Pharmaceutical Sciences, Zhengzhou University, Zhengzhou, 450000, China*

ARTICLE INFO

ABSTRACT

GB7 acetate is a *galbulimima* alkaloid obtained from *Galbulimima belgraveana*. However, information regarding its structure, biological activities, and related mechanisms is not entirely available. A series of spectroscopic analyses, structural degradation, interconversion, and crystallography were performed to identify the structure of GB7 acetate. The MTT assay was applied to measure cell proliferation on human colorectal cancer HCT 116 cells. The expressions of the related proteins were measured by Western blotting. Transmission electron microscopy (TEM), acridine orange (AO) and monodansylcadaverine (MDC) staining were used to detect the presence of autophagic vesicles and autolysosomes. A transwell assay was performed to demonstrate metastatic capabilities. Oxygen consumption rate (OCR) and extracellular acidification rate (ECAR) assays were performed to determine the mitochondrial oxidative phosphorylation (OXPHOS) and glycolysis activity of HCT 116 cells. The data showed that GB7 acetate suppressed the proliferation and colony-forming ability of HCT 116 cells. Pretreatment with GB7 acetate significantly induced the formation of autophagic vesicles and autolysosomes. GB7 acetate upregulated the expressions of LC3 and Thr172 phosphorylated adenosine 5'-monophosphate (AMP)-activated protein kinase α (p-AMPKα), which are key elements of autophagy. In addition, GB7 acetate suppressed the metastatic capabilities of HCT 116 cells. Additionally, the production of matrix metallo-proteinase-2 (MMP-2) and MMP-9 was reduced, whereas the expression of E-cadherin (E-cad) was upregulated. Furthermore, GB7 acetate significantly reduced mitochondrial OXPHOS and glycolysis. In conclusion, the structure of the novel *Galbulimima* alkaloid GB7 acetate was identified. GB7 acetate was shown to have anti-proliferative, pro-autophagic, anti-metastatic, and anti-metabolite capabilities in HCT 116 cells. This study might provide new insights into cancer treatment efficacy and cancer chemoprevention.

1. Introduction

Colorectal cancer (CRC), one of the most formidable diseases, is threatening the life and health of humans. Although colonoscopy has been introduced to screen for CRC, its incidence in both sexes is increasing [1]. In 2020, it was estimated that a total of 1,931,590 (10%) new CRC cases were diagnosed among the 19,292,789 newly diagnosed cancer cases, and 935,173 (9.4%) CRC-related deaths of 9,958,133 cancer-related deaths worldwide [2]. Diverse methods, including surgery, adjuvant radiotherapy and adjuvant chemotherapy, were used for CRC treatment. These multiple treatment options have increased the 5-year survival rate of CRC, which is still not optimistic in low-income countries [3]. Therefore, the search for efficient drugs and novel methods is considered important for the prevention and treatment of CRC.

Plant-extracted medicines in traditional Chinese medicine have been used to treat various diseases. These products have been intensively studied and display anti-cancer activities by regulating various mechanisms, including cell proliferation, apoptosis, differentiation, and metastasis, which interfere with the occurrence, progression, and development of cancer [4]. *Galbulimima belgraveana (G. belgraveana)* was first discovered in rainforests by Mueller in 1887 [5] and is widely

distributed in Papua New Guinea, Northern Australia, Indonesia, and Eastern Asia with aromatic evergreen leaves [6]. In recent decades, many active compounds from *G. belgraveana* have been reported to possess antioxidant, dormant, and analgesic properties [7]. *Galbulimima* alkaloids have received much attention because of their excellent beneficial potency. *Galbulimima* alkaloids mainly exist in the bark of *G. belgraveana* and consist of a piperidine ring and a *trans*-decalin system. *Galbulimima* alkaloids contain four classes (classes I–IV). Himbacine, as a member of class I *Galbulimima* alkaloid, has strong antagonism to muscarinic receptors, which upregulates the expression of acetylcholine and plays a positive role in treating Alzheimer's disease [8]. Natural alkaloids extracted from natural plants might be the leading compounds that have spread worldwide to promote health care and disease prevention in food application and in the pharmaceutical industry. To date, several novel *Galbulimima* alkaloids have been synthesized or purified from *G. belgraveana*. However, little information is available regarding their biological activities.

As two forms of programmed cell death (PCD), apoptosis and autophagy are important in any pathological form and mediated by intracellular procedures [9,10]. It is believed that the induction of tumor cell apoptosis with medicines or natural products is considered a useful treatment for carcinoma and other illnesses. In contrast, autophagy, which is a strictly conserved catabolic process that mediates degradation and recycling of cytoplasmic contents, is essential for the maintenance of intracellular homeostasis and elimination of defective organelles [11]. Autophagy induced by drugs might be considered beneficial for cancer patients and can suppress the proliferation of cancer cells and induce autophagic cell death (ACD) by strengthening anti-cancer treatment [12]. Induction of autophagy may be a new anti-cancer strategy.

In addition, invasion and migration affect the efficacy of chemotherapy and are regarded as prominent characteristics of cancer cells [13]. Studies have reported that approximately 50% of colorectal tumor patients might develop metastatic disease, and approximately 90% of all CRC deaths are associated with tumor metastasis, and in turn, with epithelial-mesenchymal transition (EMT) [14]. Moreover, cancer metabolic reprogramming is a characteristic of cancer [15]. Tumor cells show a high rate of glycolysis with abundant lactate production even under adequate oxygen conditions when compared to normal cells; this alteration is named "the Warburg effect" in the 20th century [16]. The high glycolysis rates allow the cells to apply the most affluent extracellular nutrients and glucose to generate sufficient ATP. Intermediate products (such as ribose, citrate and glycerol) produced by glucose degradation are needed for some biosynthetic pathways. As a result, this altered metabolism enhances acid production by tumor cells. Hence, it is regarded as a great application to study antitumor activities from the perspective of mitochondrial energy metabolism.

This study analyzed a novel *Galbulimima* alkaloid GB7 acetate extracted from *G. belgraveana* for its anti-carcinogenic effects in HCT 116 cells. The structure of GB7 acetate and its effect on HCT 116 cells were identified and investigated. In addition, the mechanisms regulating the proliferation, invasion, and migration of HCT 116 cells were studied. Our results suggest that GB7 acetate, as a novel natural product, exhibits anti-cancer activities by suppressing cell proliferation, inhibiting cell migration and invasion, and damaging mitochondrial function in HCT 116 cells.

2. Experimental

2.1. Reagents and chemicals

Trypsin, fetal bovine serum (FBS), trizol and Dulbecco's modified Eagle's medium (DMEM) were obtained from Gibco-Invitrogen (Carlsbad, CA, USA). Acridine orange (AO), monodansylcadaverine (MDC), 3-(4,5-dimethyl-2-thia-zolyl)-2,5-diphenyl-2-H-tetrazolium bromide (MTT), skim milk powder and dimethyl sulfoxide (DMSO) were purchased from Sigma-Aldrich (St. Louis, MO, USA). Phosphate-buffered saline (PBS) was obtained from HyClone (Logan, UT, USA). Primary and secondary antibodies were purchased from Cell Signaling Technology (Beverly, MA, USA). SYBR Green PCR kit was bought from Takara (Dalian, China). Seahorse XF Cell Mito Stress Test Kit, Seahorse XF Glycolysis Stress Test Kit and some related reagents were purchased from Seahorse Bioscience (North Billerica, NC, USA).

2.2. Identification of GB7 acetate

GB7 acetate was isolated and provided by Professor Lewis N. Mander at the Australian National University [6]. It was used to identify the following ways. First, layer chromatography was performed on 0.25 mm thick Merk silica gel F254 aluminum-backed plates. After brief heating by using a heat gun, ultraviolet (UV) light and/or the application of potassium permanganate solution or ninhydrin were used to visualize the results. Thereafter, flash chromatographic separations were performed on 40–63 μm silica gel 60. A Fourier transform infrared spectrometer (PerkinElmer 1800 series, Waltham, MA, USA) was used to record the infrared (IR) spectra (v_{max}). The samples were added to a KBr plate as a CDCl$_3$ solution and then air dried. An optimized automated melting point system was used to measure melting points. Subsequently, ^{13}C nuclear magnetic resonance (NMR) and ^{1}H NMR spectra were recorded at 100 MHz for carbon nuclei and 400 MHz for protons using a Bruker spectrometer. Chemical shifts were reported as internal standards at the following chemical shifts (^{13}C and ^{1}H) in parts per million (ppm) relative to the residual solvent peak: 77.0 and 7.26 ppm for CDCl$_3$. The ^{13}C NMR and ^{1}H NMR spectra are reported as follows: chemical shift, coupling constant (Hz), multiplicity (s: singlet; d: doublet; t: triplet; q: quartet; p: pentet; qd: quartet of doublets; br: broad; and m: multiplet), integration, and assigned position. High-resolution electrospray ionization (ESI) mass spectra were recorded using a time-of-flight instrument, and low-resolution measurements were recorded using a single quadrupole liquid chromatography-mass spectrometer. Subsequently, a magnetic sector machine was used to record the electrospray ionization mass spectra.

2.3. Cell culture

Human colorectal cancer HCT 116 cells were obtained from American Type Culture Collection (Manassas, VA, USA). HCT 116 cells were cultured with DMEM supplemented with 10% FBS, penicillin (100 U/mL) and streptomycin (100 μg/mL) in a humidified atmosphere at 37 °C and 5% CO$_2$.

2.4. MTT assay

The viability of HCT 116 cells was detected using MTT assay. The cells were placed in 96-well plates (8×10^3 cells/well) for overnight, and then treated with 12.5–200 μg/mL GB7 acetate or without GB7 acetate for 24 h. And 20 μL of MTT (5 mg/mL) was added into each well and cultured for another 4 h. DMSO was then added to dissolve MTT tetrazolium crystals. The plate was placed on an enzyme immunoassay detector and shaken for 10 min under low-speed oscillation. The absorbance was obtained at an optical density (OD) of 490 nm. The cell viability was determined using the following formula:

$$\text{Cell viability } (\%) = (OD_{490(sample)} - OD_{490(blank)}) \, / \, (OD_{490(control)} - OD_{490(blank)}) \times 100$$

2.5. Colony formation assay

HCT 116 cells pretreated with GB7 acetate (0, 50, 100, and 150 μg/mL) were seeded into a 6-well plate. After two weeks of cultivation, HCT 116 cells were gently washed twice, and stained with 0.1% crystal violet. Colonies composed of more than 50 cells were counted. The colony-forming efficiency was analyzed by dividing the number of colonies formed in the treatment group by that in the control group.

2.6. Western blotting

After HCT 116 cells were treated with GB7 acetate, the cells were lysed with RIPA solution (Bestbio, Shanghai, China) containing protease inhibitor (Bestbio, Shanghai, China) and phosphatase inhibitor (Bestbio, Shanghai, China). The total protein was collected by centrifugation at 14,000 g for 15 min. The protein samples (50 μg) were subjected to 10% sodium dodecyl sulfate (SDS)-polyacrylamide gel electrophoresis (PAGE), separated under 80 V, and transferred onto polyvinylidene fluoride (PVDF) membranes (Bio-Rad Laboratories). The membranes were then incubated with primary antibody and secondary antibodies to probe the target proteins, such as microtubule-associated protein 1 light chain 3 (LC3), poly ADP-ribose polymerase (PARP), caspase-3, E-cadherin (E-cad), matrix metallo-proteinase-2 (MMP-2), and MMP-9. In the last step, the membranes were visualized using a chemiluminescence detection kit (Pierce Biotechnology, Rockford, IL, USA) according to the manufacturer's instructions. The target protein was normalized to glyceraldehyde-3-phosphate dehydrogenase (GAPDH), which was used as a loading control.

2.7. Annexin V-fluoresceine isothiocyanate (FITC)/propidium iodide (PI) staining assay

After incubation with GB7 acetate (from 12.5 to 200 μg/mL), the cells were washed, trypsinized, and collected. Apoptotic rate was detected using an Annexin V-FITC/PI detection kit (BioVision, San Francisco, CA, USA) according to the manufacturer's protocol. Finally, flow cytometry (BD Biosciences, New York, USA) was used to stain and analyze at least 10,000 cells.

2.8. AO and MDC staining

Autophagic vacuoles are hallmarks of autophagy. AO and MDC staining methods were used to observe autophagic vacuole and autophagosome formation in HCT 116 cells. HCT 116 cells were individually seeded into 6-well plates overnight, and then treated with 100 μg/mL GB7 acetate for 24 h. AO (1 μg/mL) and MDC (0.05 mM) were added to each well to stain cells for 15 min and 60 min. After washed with PBS three times, HCT 116 cells were photographed using a fluorescence microscope (Olympus, IX-73, Tokyo, Japan).

2.9. Transmission electron microscope

After exposure to 100 μg/mL GB7 acetate for 24 h, HCT 116 cells were treated with precooled glutaraldehyde (2.5%) for 30 min, and then fixed in osmium tetroxide for embedding in Spurr's Epon. The ultrathin sections were obtained to observe autophagy lysosomes using a Hitachi 7500 electron microscope.

2.10. Wound healing assay

HCT 116 cells were seeded into a 6-well plate. After reaching 90% confluence, the attached cells were removed using a plastic pipette tip to form a single wound in the center of the well. The cells were then treated with GB7 acetate (0, 50, 100, and 150 μg/mL) and photographed at 0, 24, and 48 h with a fluorescence microscope (Olympus, IX-73, Tokyo, Japan). The wound closure area was calculated using the following formula:

$$\text{Migration area } (\%) = (M_0 - M_n) \, / \, M_0 \times 100\%$$

where M_0 represents the wound area at the beginning, and M_n represents the wound area at the measurement point.

2.11. Transwell assay

After cultured in low serum (5% FBS) medium, HCT 116 cells were seeded into the upper chamber of a transwell 24-well plate with 8 μm pore filters. GB7 acetate was added into the lower chamber for 24 h. And the migrated cells on the lower surface were stained with 0.5% crystal violet for 5 min. Finally, an optical microscope (Olympus, IX-73, Tokyo, Japan) was used to observe migration.

2.12. Invasion assay

For matrigel invasion assays, the matrigel and DMEM pre-cooled medium were mixed thoroughly at a 1:5 ratio. The mixture (50 μL) was added to the upper compartments of 24-well plates and placed in an incubator for 4 h to cure the matrigel. The upper chamber was filled with 200 μL of the cell suspension without serum. Complete medium was added to the lower chamber as a chemoattractant and supplemented with GB7 acetate (0, 50, 100, and 150 μg/mL). The invaded cells on the lower surface were fixed with 4% paraformaldehyde, stained with 0.5% crystal violet, photographed and counted.

2.13. Oxygen consumption rate (OCR) and extracellular acidification rate (ECAR)

The mitochondrial bioenergetics of HCT 116 cells, in response to GB7 acetate (0, 50, 100, and 150 μg/mL), was assessed using a Seahorse Bioscience XFP Extracellular Flux Analyzer (Seahorse Bioscience, Boston, MA, USA). To determine OCR, the optimal cell number for each OCR measurement was seeded at 30,000 cells/well. After treated with different concentrations of GB7 acetate, HCT116 cells were cultured overnight. On the second day, the medium was replaced with unbuffered DMEM supplemented with glucose (25 mM), glutamine (1 mM) and sodium pyruvate (1 mM); and the cells were equilibrated without CO_2 for 1 h. Thereafter, the following chemicals were injected into the medium and OCR was measured: (a) oligomycin (OM; 10 μM), an ATP synthase inhibitor; (b) p-trifluoromethoxy carbonyl cyanide phenylhydrazone (FCCP; 0.25 μM), an accelerator that leads to maximum respiratory rate; (c) a mixture of rotenone (ROT) and antimycin A (AA) (5 μM) and mitochondrial complex I and III inhibitors, respectively. To measure ECAR, GB7 acetate pretreatment was the same as the OCR determination. Glucose (10 mM), oligomycin (10 μM), and 2-DG (50 mM) were sequentially injected to detect glycolysis, glycolytic capacity and glycolytic reserve. Seahorse Wave software was used to analyze all the XFP results. OCR and ECAR were estimated as pmol/min and pmH/min, respectively. Each study was conducted at least three times.

2.14. Statistical analysis

All data are shown as mean ± SD. One-way analysis of variance (ANOVA) and Duncan's multiple-range test were used to perform statistical analysis. Statistical significance was set at $P < 0.05$.

3. Results

3.1. Isolation and identification of the GB7 acetate from the bark of G. belgraveana

Similar to the *Galbulimima* alkaloids found to date, a new compound, 7 (GB7 acetate), was isolated from the bark of *G. belgraveana*. GB7 acetate was obtained as a yellow solid amorphous by recrystallization from the elution in different proportions of methanol/dichloromethane/NH_3, m.p.: 101–102 °C, specific rotation $[\alpha]_D^{20} = +44.86$ (c 3.3, CHCl$_3$). ^{1}H NMR (400 MHz, CDCl$_3$) : δ 7.97 (d, $J = 6.9$ Hz, 2H), 7.52 (t, $J = 7.4$ Hz, 1H) 7.40 (t, $J = 7.6$ Hz, 2H) 6.04 (d, $J = 7.9$ Hz, 1H), 5.39 (s, 1H), 3.58 (s, 3H), 3.50 (m, 1H), 3.33 (m, 1H), 3.11 (s, 3H), 3.09 (m, 1H), 2.94–2.86 (complex m, 1H), 2.78 (m, 1H), 2.51 (d, $J = 11.0$ Hz, 1H), 2.46–2.34 (complex m, 1H), 2.29 (m, 1H), 2.14–2.04 (complex m, 1H), 2.02 (s, 3H), 1.97 (s, 3H), 1.93–1.84 (complex m, 2H), 1.84–1.74 (complex m, 2H), 1.73–1.65 (complex m, 2H), 1.54 (d, $J = 7.2$ Hz, 3H), 1.45–1.30 (complex m, 2H) (Fig. 1A); ^{13}C NMR (100 MHz, CDCl$_3$): δ170.3, 168.9, 168.0, 165.9, 149.0, 132.5, 130.9, 129.5 (x2), 128.2 (x2), 116.9, 86.1, 85.1, 72.5, 69.2, 66.7, 63.6, 57.0, 55.5, 51.5, 49.6, 42.7, 42.1, 41.9, 39.9, 37.1, 27.9, 26.4, 25.5, 23.4, 21.4, 21.3, 20.9 (Fig. 1B). IR (KBr, cm^{-1}): ν$_{max}$ 2933, 2865, 1734, 1449, 1369, 1317, 1266, 1243, 1177, 1110, 1064, 1026, 954, 892, 754, 712 cm^{-1} (Fig. 1C). The molecular formula of GB7 acetate was

recognized as C$_{34}$H$_{41}$NO$_9$, based on the electron ionization mass spectrometry (HREIMS) peak at *m/z* 608.5 ([M+H]$^+$, 100%) (Fig. 1D); HRMS M$^{+\cdot}$ calculated for C$_{34}$H$_{41}$NO$_9$: 608.2854, found: 608.2871. These data revealed the structure of GB7 acetate (Fig. 1E).

3.2. GB7 acetate suppressed the viability and colony-forming of HCT 116 cells

To examine whether GB7 acetate treatment affects the proliferation and clonogenicity of HCT 116 cells, MTT assay and colony formation assay were performed to detect the growth of tumor cells. Compared with the control group, the proliferation of HCT 116 cells was suppressed after treatment with GB7 acetate for 24 h (Fig. 2A). The viability of HCT 116 cells showed a significant decrease ($P < 0.05$) after treatment with GB7 acetate (from 25 to 200 μg/mL) and the half maximal inhibitory concentration (IC$_{50}$) value was 97.75 ± 6.56 μg/mL. Colony formation assays further showed that GB7 acetate significantly suppressed the colony-forming efficiency of HCT 116 cells in the 100 μg/mL group (11.60% ± 3.74%) after treatment for two weeks when compared with the control group (45.40% ± 10.21%) ($P<0.001$) (Figs. 2B and C). These results indicated that GB7 acetate significantly inhibited proliferation and attenuated the colony-forming ability of colorectal cancer cells in vitro.

3.3. GB7 acetate did not induce apoptosis in HCT 116 cells

Apoptosis is considered as a significant physiological event that targets antitumor agents and cancer treatment [17]. Apoptosis plays a vital role in intercellular homeostasis and individual
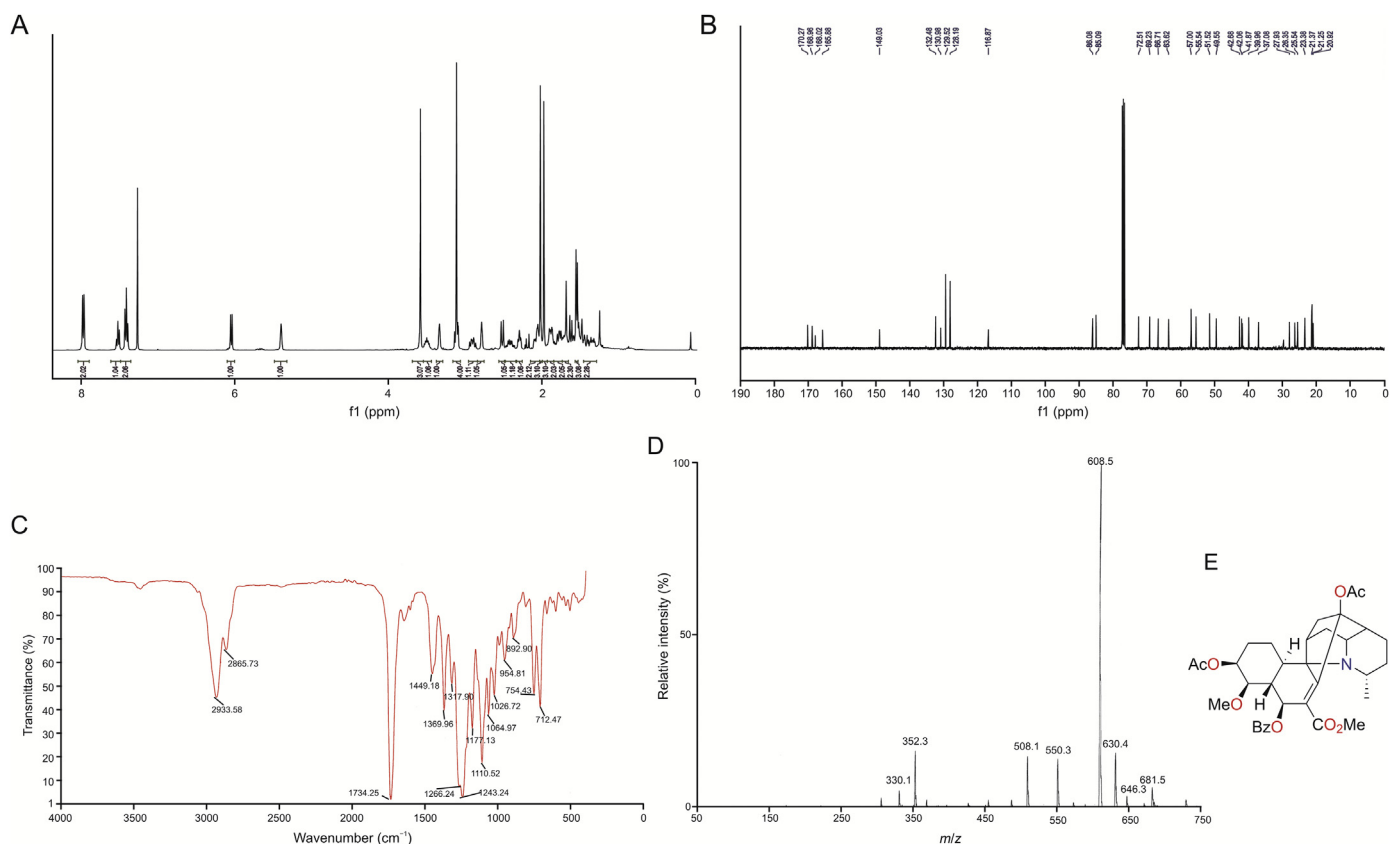

Fig. 1. Structural identification of GB7 acetate. (A) The ^{1}H NMR and (B) ^{13}C NMR spectra of GB7 acetate. (C) The IR (KBr) data of GB7 acetate. (D) MS analysis of GB7 acetate. (E) The structure of GB7 acetate.
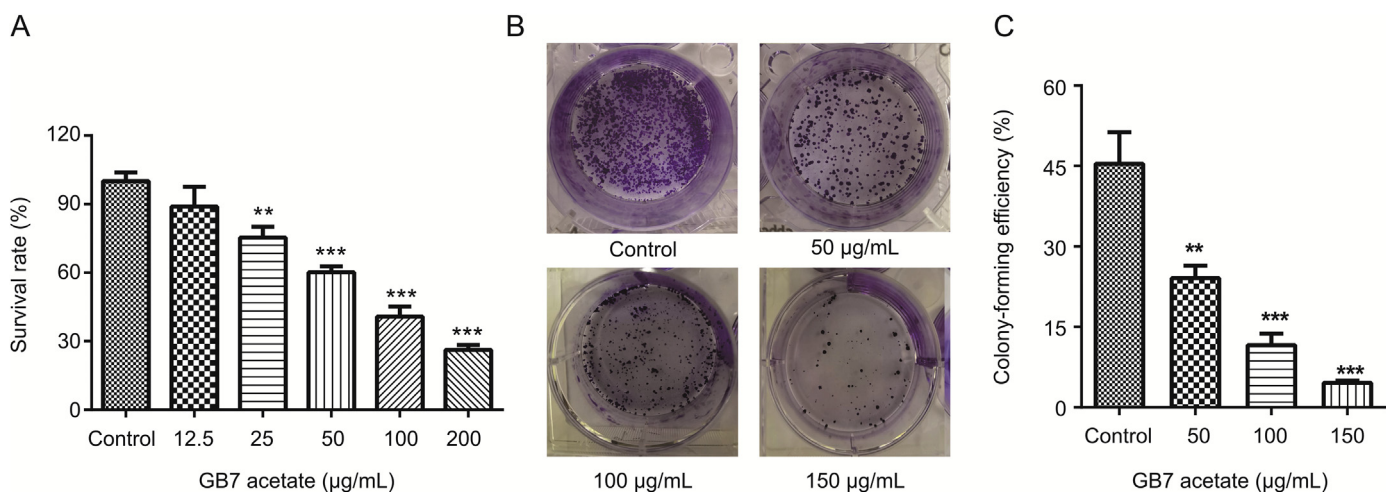
Fig. 2. GB7 acetate inhibited proliferation and colony formation of HCT 116 cells. (A) The cell viability detected by MTT assay after HCT 116 cells treated with GB7 acetate (12.5−200 μg/mL) for 24 h. (B) Colony formation. The HCT 116 cells at a density of 1000 cells in 6-well plates were seeded and cultured for 24 h before treatment with 50, 100, and 150 μg/mL of GB7 acetate, followed by culturing for 14 days. (C) Histogram of colony-forming efficiency in response to the GB7 acetate treatment. Data are presented as means ± SD ($^{**}P<0.01$, $^{***}P<0.001$ vs. control).

development [18]. The effect of GB7 acetate on the expressions of cleaved PARP and cleaved caspase-3 in HCT 116 cells was investigated. As shown in Fig. 3A, the activated form of PARP and caspase-3 did not appear in HCT 116 cells treated with GB7 acetate for 24 h. Moreover, GB7 acetate showed no significant effects on the expressions of PARP and caspase-3 in HCT 116 cells. Annexin V-FITC/PI staining assay was used to quantitatively analyze the apoptotic rate after treatment with GB7 acetate for 24 h. As shown in Fig. 3B, the percentages of early and late apoptosis were less than 10% when treated. Moreover, the apoptotic rates in the GB7 acetate groups showed no significant changes when compared to those in the control group (Fig. 3C). These findings demonstrated that GB7 acetate showed no significant pro-apoptotic effects on HCT 116 cells.

3.4. GB7 acetate induced autophagy mainly via AMPK signaling pathway in HCT 116 cells

The effect of GB7 acetate on autophagy in HCT 116 cells was investigated to further study the mechanism of the anti-proliferative activity of GB7 acetate. In AO staining cells, bright green and deep red fluorescence appeared in the cytoplasm and nucleolus, whereas the acid zone glowed bright red [19]. The autofluorescent drug MDC is a selective hallmark to evaluate acidic vesicular organelles (AVOs), such as autophagic vacuoles and autolysosomes [20]. As shown in Fig. 4A, AVOs (red fluorescence) formation in the GB7 acetate groups was significantly more than that in the control group. Similarly, the number of MDC-labeled fluorescent dots also increased after treatment with GB7 acetate (Fig. 4B), suggesting that GB7 acetate enhanced the formation of autolysosomes.

To further investigate the activation of autophagy in HCT 116 cells by GB7 acetate, internal changes in HCT 116 cells were examined by TEM. The cells without treatment with GB7 acetate consisted of dense cytoplasm and well-preserved organs, prominent nucleoli, convoluted and large nuclei, and dispersed chromatin. Small empty vacuoles were observed in the cytoplasm. Vacuolar structures surrounded by dense membranes were seen in the cytoplasm of cells exposed to GB7 acetate for 24 h. Autophagosomes containing materials of different structures and digested organelles were also seen in HCT 116 cells (Fig. 4C). The details of

cytoplasmic portions are shown. These results suggested that GB7 acetate induced cell autophagy in HCT 116 cells.

LC3 plays a vital role in autophagosomes and is considered as a marker of autophagy [21]. The transition of LC3-I to LC3-II is a key step in the progression of autophagy in mammalian cells [22]. As shown in Figs. 4D and E, the expression of LC3-II was upregulated in a concentration-dependent manner in HCT 116 cells after treatment with GB7 acetate for 24 h. The above data clearly suggested that GB7 acetate induced autophagy in HCT 116 cells through the induction of LC3 conversion. AMPK, a cell energy state sensor, is triggered by high intracellular AMP, thereby activating autophagy through the mammalian target of rapamycin (mTOR)-related pathway [23]. To explore the possible mechanism of GB7 acetate-induced autophagy in HCT 116 cells, the expression of AMPK was analyzed. The results showed that Thr172 phosphorylated AMPKα (p-AMPKα) was significantly enhanced in HCT 116 cells after treatment with GB7 acetate (Figs. 4D and F), suggesting that GB7 acetate-induced autophagy mainly occurred through AMPK-related signaling pathways.

3.5. GB7 acetate reduced the mobility and invasion of HCT 116 cells

Metastasis and invasion are the distinguishing features of malignant neoplasms, resulting in clinical death in most patients with tumors. Wound healing assay and transwell assay were performed to investigate the effects of GB7 acetate on the migration and invasion capacities of HCT 116 cells. The wound healing assay showed that GB7 acetate significantly decreased the migration area of HCT 116 cells when compared with the control group ($P<0.05$) (Figs. 5A and B). Wound healing of 34%−43% was observed after 24 h and 48 h in untreated cancer cells, whereas 10%−21% were seen in the 100 and 150 μg/mL GB7 acetate groups.

Furthermore, the transwell migration assay confirmed that GB7 acetate distinctly reduced the migratory capacity of HCT 116 cells, because the number of cells migrating to the other side was markedly lower in the 50, 100, and 150 μg/mL groups than in the control group ($P<0.05$) (Figs. 5C and E). The results of the matrigel-based invasion assay showed that the cell invasion rate was significantly decreased in the GB7 acetate group when compared with the control group ($P<0.05$) (Figs. 5D and F). These findings
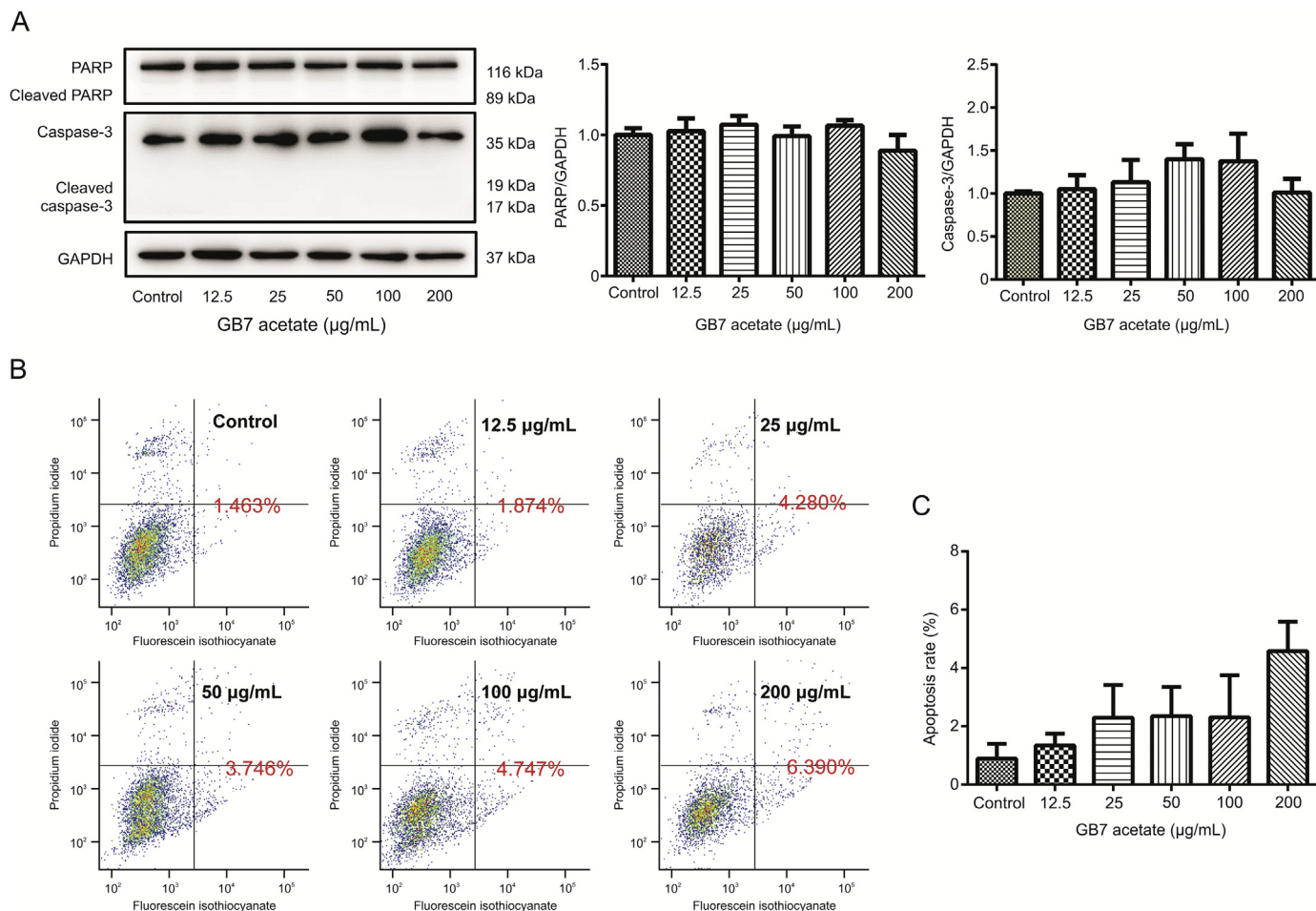
Fig. 3. Effects of GB7 acetate on cleavage of PARP, caspase-3 and apoptosis rate in colorectal cancer cells. (A) Expressions of PARP and caspase-3 in HCT 116 cells detected by Western blotting after treatment with GB7 acetate for 24 h. (B) Apoptotic rate examined by flow cytometry, and (C) a histogram of apoptotic rate in HCT cells after treatment with GB7 acetate for 24 h. Data are shown as means ± SD (n=3). One-way ANOVA was carried out to compare the differences. (Note: LR + UR were considered as apoptosis.)

demonstrated that the motility and invasiveness of HCT 116 cells were clearly suppressed following GB7 acetate treatment in vitro.

Enhancement of cancer cell mobility is essential for metastatic processes. For cancer cells to migrate, the cells need to change their behavior. The mean expression of E-cad suggests that GB7 acetate might regulate EMT. To test this hypothesis, the expression of E-cad was analyzed by Western blotting and it was found that GB7 acetate after 24 h treatment significantly upregulated the expression of E-cad in HCT 116 cells (Fig. 5G).

Matrix metalloproteinases (MMPs), such as MMP-2 and MMP-9, play an important role in tumor invasion and metastasis [24]. The expressions of MMP-2 and MMP-9 were then determined, and the findings showed that the expressions of MMP-2 and MMP-9 were gradually reduced by GB7 acetate treatment (Figs. 5H and I). These results suggest that GB7 acetate might inhibit the migratory ability of HCT 116 cells by modulating the activity of E-cad and suppressing the expressions of MMP-2 and MMP-9 to stop extracellular matrix (ECM) degradation and suppress cancer invasion and metastasis.

3.6. Effects of GB7 acetate on mitochondrial oxidative phosphorylation (OXPHOS) as well as glycolysis

Furthermore, the effect of GB7 acetate on mitochondrial metabolism was explored. ATP is produced through mitochondrial

respiration and aerobic glycolysis. The OCR suggesting mitochondrial OXPHOS activity and ECAR indicating lactic acid production were monitored in real time using an XF96 extracellular flux analyzer. Multiple studies have shown a correlation between mitochondrial function and tumors. The results revealed that the overall OCR was suppressed by GB7 acetate treatment in HCT 116 cells (Fig. 6A). To elucidate the effect of OCR by GB7 acetate treatment, we evaluated four mitochondrial respiration indicators, namely, basal respiration rate, maximum respiration rate, ATP production and spare respiratory capacity. We found that the basal respiration rate and the maximum respiration rate, ATP production, and spare respiratory capacity were all decreased in GB7 acetate-treated cells (Figs. 6B−E). In addition, as shown in Fig. 6F, overall glycolysis was significantly reduced in GB7 acetate treated HCT 116 cells. Glycolysis, glycolytic capacity, and glycolytic reserve were also assessed. Significant reductions in these three indices were found in HCT 116 cells (Figs. 6G−I). These findings suggest that GB7 acetate has an inhibitory effect on mitochondrial OXPHOS and glycolysis.

4. Discussions

Medicinal herbs contain several beneficial compounds and have been extensively used to identify novel compounds that may show therapeutic effects in treating various diseases. For example,
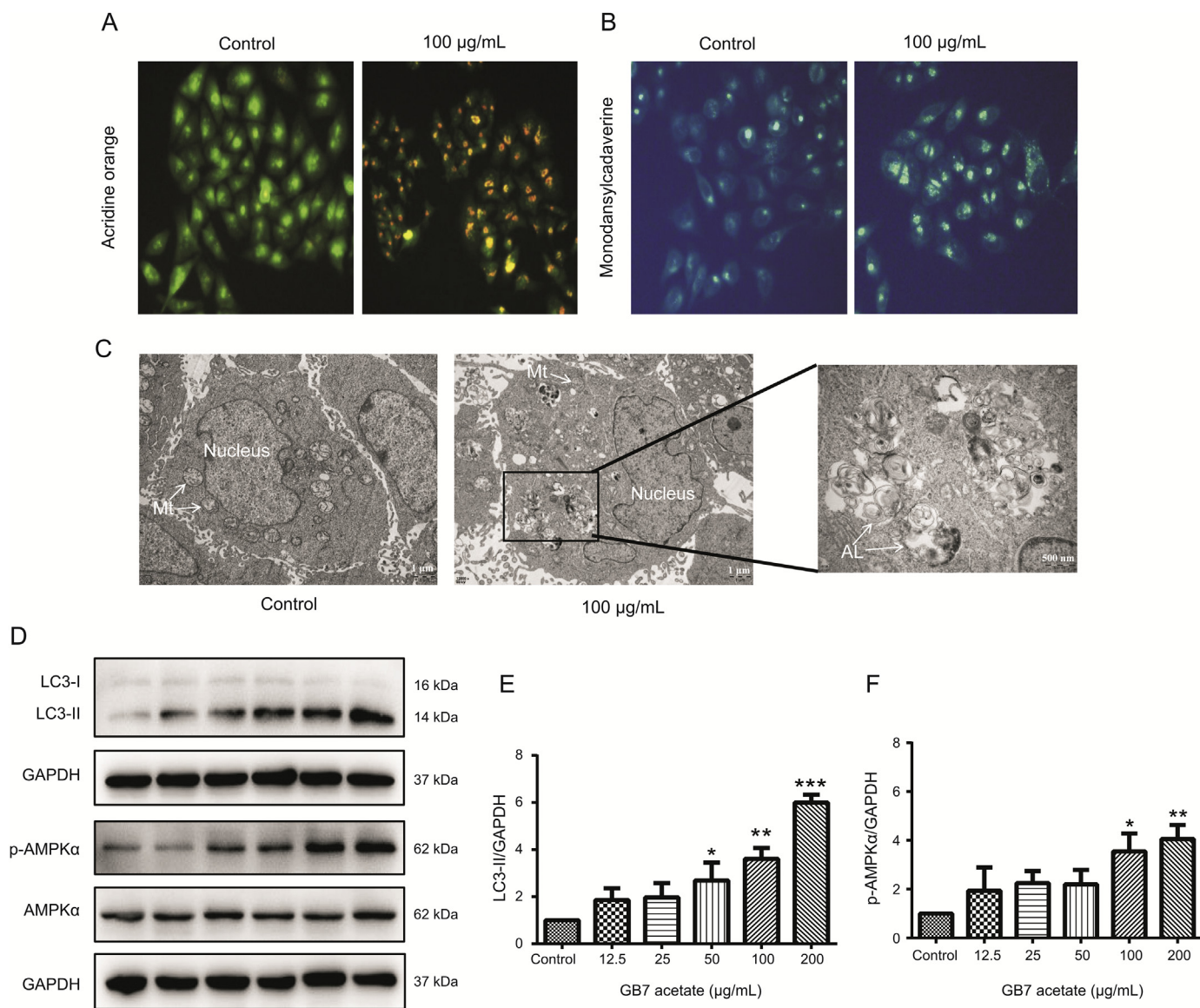
Fig. 4. Effects of GB7 acetate on autophagy activation in colorectal cancer HCT 116 cells. The accumulation of autophagic vacuoles in HCT 116 cells using (A) AO and (B) MDC staining after treatment with 100 μg/mL GB7 acetate for 24 h. (C) Electron microscopy analysis of micromorphology changes of HCT 116 cells after treatment with GB7 acetate for 24 h. (D) Western blotting analysis of LC3-II and p-AMPKα expression in HCT 116 cells after GB7 acetate treatment. GAPDH was used as a loading control. (E and F) Histograms of the expressions of LC3 II and p-AMPKα of HCT 116 cells. Data are shown as means ± SD ($n=3$). One-way ANOVA was performed to compare the difference. $^*P<0.05$, $^{**}P<0.01$, $^{***}P<0.001$ vs. control. Mt: mitochondrion; AL: autolysosomes.

epigallocatechin gallate from green tea, myricetin and quercetin from dietary herbs suppress cell proliferation and differentiation [25], emphasizing the need to identify novel compounds that affect tumor progression in a non-toxic manner. GB7 acetate, a novel *Galbulimima* alkaloid, was identified, and its structure and biological activity were identified. The results of this study demonstrated that GB7 acetate possessed anti-cancer activity by inhibiting cell proliferation and colony formation, weakening the invasiveness and migratory capabilities, and modulating mitochondrial OXPHOS and glycolysis in HCT 116 cells. These results may serve as a theoretical basis for identifying natural compounds that enhance cancer treatment efficacy or cancer chemoprevention.

PCD, including apoptosis and autophagy, occurs in any pathological forms mediated by intracellular procedures. The apoptotic signaling pathway is divided into two major pathways, the endogenous and exogenous pathways, and is also called the mitochondrial pathway and receptor-mediated cell death. Although the initial events of these two apoptotic signaling pathways are different, they eventually induce apoptosis by activating the caspase effect. PARP, an early sign of apoptosis, is widely considered as an endogenous substrate of caspase-3 [26]. Autophagy serves as a "self-phagocytosis" and dynamic process that engulfs cytoplasmic proteins, alters organelles or complexes into autophagosome (double-membrane-double structure), degrades, and recycles. Several studies [27,28] indicated that autophagy might be another mechanism of cell death, which is regarded as ACD, and highlights the potentially lethal effect of autophagy. ACD is characterized by a lack of chromatin condensation, accumulation of cytoplasm vacillations, caspase-independent apoptosis, and LC3 lipidation. It is usually inhibited by autophagy pathway blockers or knockout of the core autophagy genes [29]. Studies have indicated that the anti-proliferative activities of alkaloid compounds (including Harmol and Hernandezine) [26,30] are
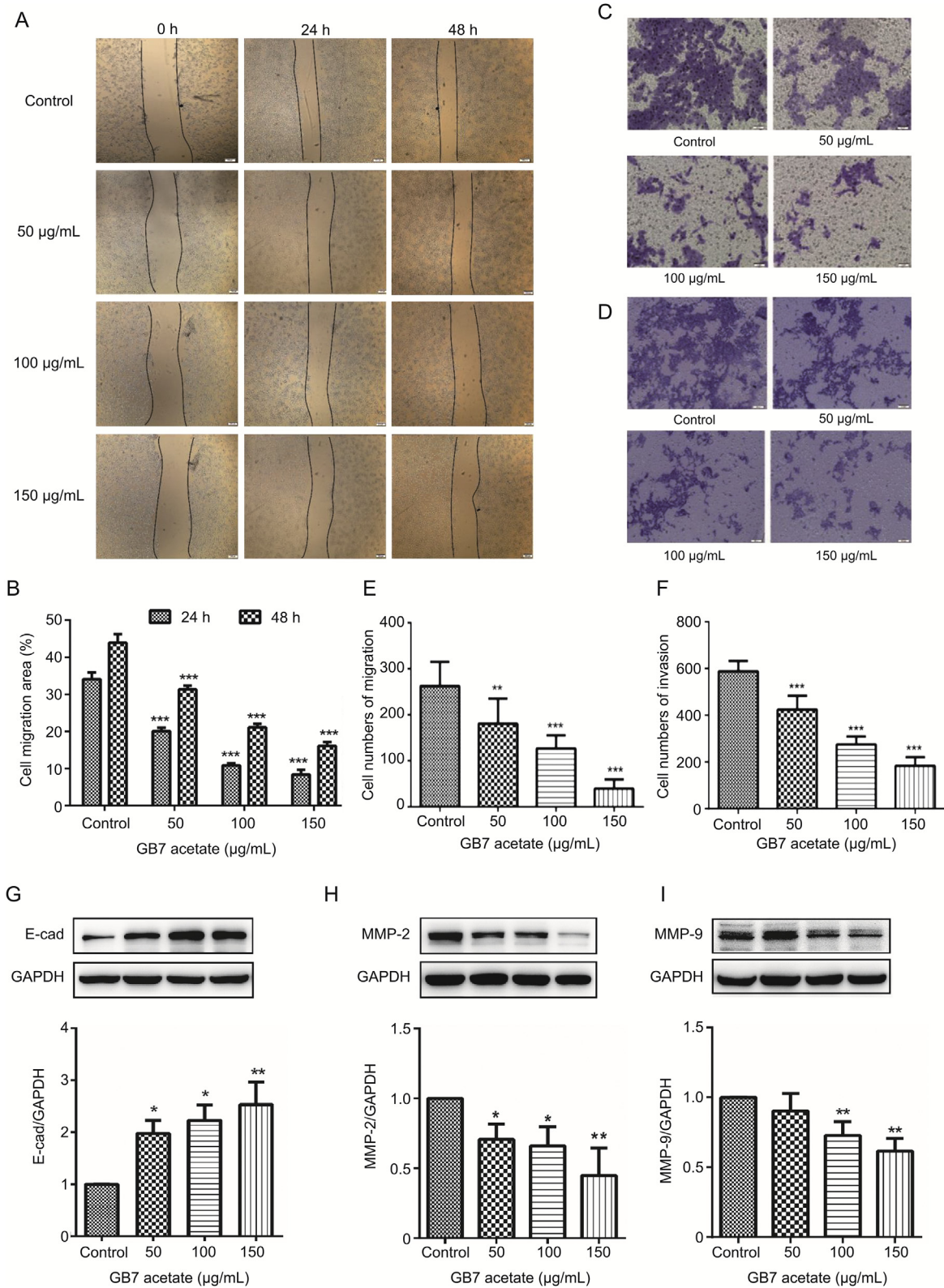
Fig. 5. GB7 acetate decreased the motility and invasiveness of HCT 116 cells and affected the expressions of E-Cad, MMP-2 and MMP-9. (A) Scratch wound healing assays of rate of cell migratory area in GB7 acetate treatment groups and control group at 0, 24, and 48 h. (B) Rate of cell migratory area. (C) Migration and (D) invasion of HCT 116 cells stained with crystal violet after GB7 acetate treatment for 24 h. (E and F) Histograms of the cell numbers of migration and invasion in the bottom chamber. (G—I) Protein expressions of E-cad (G), MMP-2 (H) and MMP-9 (I) using Western blotting after HCT 116 cells exposure to 50, 100, and 150 μg/mL GB7 acetate for 24 h. The data are presented as means ± SD of three independent experiments ($^{*}P<0.05$, $^{**}P<0.01$, $^{***}P<0.001$ vs. control).
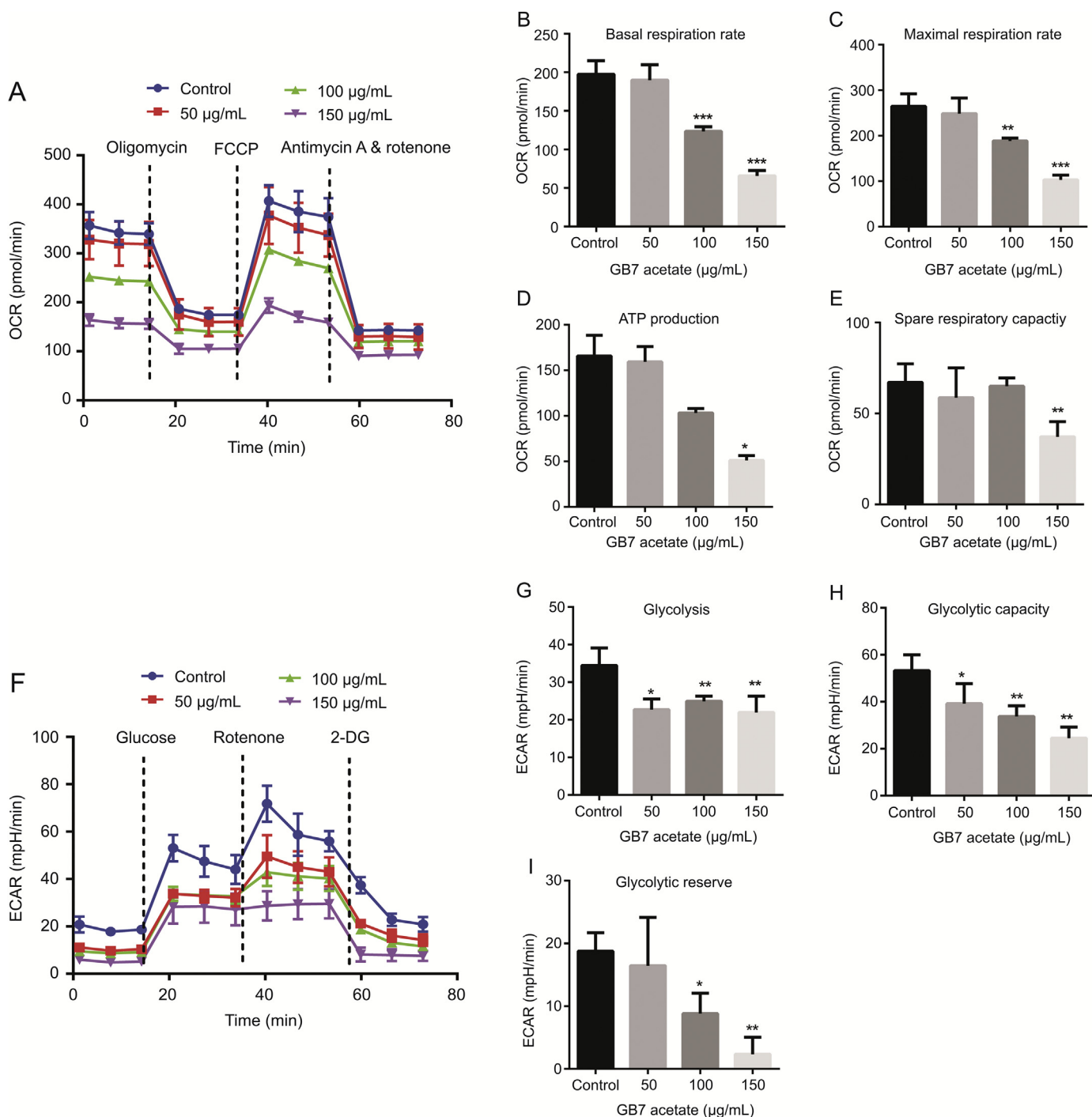
Fig. 6. GB7 acetate decreased mitochondrial respiration and glycolysis in HCT 116 cells. (A) Real time overall OCR of HCT 116 cells treated with GB7 acetate of different concentrations (50, 100, and 150 μg/mL) for 24 h was detected through the Seahorse XF96 Extracellular Flux analyzer. (B) Basal respiration rate, (C) maximal respiration rate, (D) ATP production, and (E) spare respiratory capacity associated OCR of HCT 116 cells treated by GB7 acetate of various concentrations. (F) Real time overall ECAR of HCT 116 cells treated with GB7 acetate of various concentrations (50, 100, and 150 μg/mL) for 24 h by the Seahorse XF96 Extracellular Flux analyzer. (G) Glycolysis, (H) glycolytic capacity, and (I) glycolytic reserve of HCT 116 cells treated with GB7 acetate of various concentrations. The data are presented as means ± SD of three independent experiments ($^*P<0.05$, $^{**}P<0.01$, $^{***}P<0.001$ vs. control).

mainly induced through cell apoptosis and/or autophagy. In this analysis, GB7 acetate did not activate PARP and caspase-3, and change the rate of apoptotic cells in HCT 116 cells. However, GB7 acetate showed strong activity in autophagy by enhancing autolysosome and autophagosome formation and increasing the expression of LC3-II in a concentration-dependent manner in HCT 116 cells. These findings demonstrated that GB7 acetate induced the anti-

proliferative activities mainly through induction of cell autophagy rather than apoptosis.

There is a complex and diverse connection between apoptosis and autophagy, which ensures that cells can balance life and death when responding to various stress stimuli [9]. In some cases, autophagy inhibits apoptosis, which is a way for cells to survive. However, autophagy itself can also induce cell death. It can act

together with apoptosis and act as a backup mechanism to induce cell death in the case of apoptotic defects. In recent years, some studies targeting the autophagy pathway have shown that promoting ACD or inhibiting autophagy protection is an effective way to fight tumors and counteract chemotherapy resistance [27,28].

In addition, we confirmed the possible mechanism of GB7 acetate-induced autophagy. As a result, p-AMPKα was significantly increased in HCT 116 cells after GB7 acetate treatment. mTOR is regarded as a downstream target of AMPK, which serves as a common intracellular nutrient sensor. A previous study also indicated that AMPK induces autophagy by enhancing the mammalian autophagy-initiated kinase unc-51-like kinase 1 (ULK1) under special conditions; however, high mTOR activity blocks the trigger of ULK1, interfering with the relationship between AMPK and ULK1 [31]. Although the molecular mechanism that supports alkaloid to induce cell death remains unclear, some studies have demonstrated that these alkaloids (berberine, hernandezine, cepharanthine, iso-liensinine, dauricine, and liensinine) activate the AMPK signaling cascade [26,32]. Other natural products including coenzyme Q (CoQ) and polyphenols are related to the AMPK signaling pathway, and then activate two upstream kinases AMPK signaling through hepatic kinase B1 (LKB1) and Ca^{2+}-stimulated kinase (CaMKK) to treat different diseases [33]. Moreover, LC3-II is found to increase after GB7 acetate treatment, and the expressions of Beclin-1 and LC3-II might also directly activate autophagy. Therefore, the possible molecular mechanism of GB7 acetate-induced autophagy might mainly involve the AMPK signaling pathway by activating LKB1 or CaMKK upstream kinases and directly enhancing the level of Beclin-1 and LC3-II to induce autophagy.

The migration of tumor cells is a multi-step and continuous process. Furthermore, our study results demonstrated that GB7 acetate inhibited proliferation and colony formation in HCT 116 cells, suggesting its anti-cancer activity. It has been reported that alkaloids suppress cell viability, invasiveness, and migratory capabilities in many cancer cells. Kuo et al. [34] demonstrated that berberine significantly inhibits the metastasis of squamous tumor cells. Similar results were found in a breast carcinoma cell study [14]. The results of this study indicated that the invasiveness and migratory capabilities of HCT 116 cells were significantly weakened by subsequent treatment with GB7 acetate.

Most CRC deaths are associated with tumor metastasis, usually related to EMT [35,36]. E-cad, a protein regulated during EMT, is known to be decreased to enhance cancer metastasis [37]. In addition, MMPs are responsible for remodeling ECM and play an important role in cancer progression. The ECM, an important modulated component in cell physiology, provides a suitable environment for cell migration. MMPs have been implicated in CRC invasion and metastasis, particularly MMP-2 and MMP-9 [38]. Therefore, suppression of MMP expression may be regarded as an early target to prevent carcinoma metastasis. This study revealed that GB7 acetate acted as a potent inhibitor of EMT by increasing E-cad and significantly decreasing the level of MMP-2/MMP-9 in HCT 116 cells. This result suggested that GB7 acetate can be a moderator of ECM breakdown during cancer metastasis and invasion because of its ability to modulate the production of MMP. This study provides data to consider that GB7 acetate might be effective in suppressing cancer cell metastasis and invasion.

Moreover, tumor cells readjust their metabolism by promoting growth, proliferation, and long-term homeostasis. The common characteristics of this metabolic change include increased glucose uptake and glucose fermentation by lactic acid. This phenomenon is found in fully functional mitochondria and is called the Warburg effect [16]. In addition, several studies have demonstrated that most of the tumor mitochondria are not damaged when performing mitochondrial OXPHOS. They have been reprogrammed to provide the needs of macromolecular biosynthesis and human cancer growth [39]. To satisfy the energy requirements of cell invasion, invadopodia are removed from the forefront of cancer cells [40]. In recent years, several alkaloids have exhibited greater potential in tumor research. Many alkaloids have antitumor activities and selectively affect specific functions of cancer mitochondria through suppression of mitochondrial metabolic pathways, regulation of OXPHOS, metabolic transportation, and mitochondria-dependent apoptosis [41]. Increased dependence on glycolysis due to mito-chondrial changes in tumor cells is considered to be the biochemical basis for the preferential elimination of cancer cells with appropriate glycolytic inhibitors. López-Lázaro [42] revealed that digi-toxin, a cardiac drug, suppresses cell viability and induces apoptosis through suppressing glycolysis in tumor cells. Sanguinarine is an alkaloid that exerts anti-proliferative activity against several types of human cancer cell lines and demonstrates its effect on the cell mitochondrial respiratory chain and the calcium load capacity [43]. In various types of cancer cells, particularly in clonal cells with damaged mitochondrial respiration, inhibitory effects on glycolysis were observed to induce marked ATP depletion. In addition, significant inhibition of tumor migratory cells was observed because of an inadequate supply of ATP. The continuous acidity of the tumor microenvironment causes tumor cells to invade other normal tissues [44]. In this study, GB7 acetate showed strong inhibitory effects on mitochondrial OXPHOS and glycolysis. The results suggest that GB7 acetate may have potential applications in tumor therapy.

5. Conclusion

This study revealed the structure, the antitumor effects, and the related mechanisms of the novel natural compound GB7 acetate from *G. belgraveana*. This study showed that GB7 acetate had anti-proliferative effects on HCT 116 cells and induced autophagy via the AMPK signaling pathway. Furthermore, GB7 acetate significantly inhibited HCT 116 cells metastasis and suppressed metabolic capabilities. This was the first study to identify the structure of GB7 acetate and its role as an inhibitor of HCT 116 cells. These results might be helpful in identifying natural compounds that enhance cancer treatment efficacy or cancer chemoprevention in the future.

CRediT author statement

Ziyin Li: Validation, Investigation, Writing - Original draft preparation; **Lianzhi Mao**: Formal analysis, Investigation; **Bin Yu**: Validation, Formal analysis; **Huahuan Liu** and **Qiuyu Zhang**: Conceptualization, Methodology, Resources; **Zhongbo Bian:** Conceptualization, Resources; **Xudong Zhang:** Investigation, Data curation; **Wenzhen Liao** and **Suxia Sun**: Writing - Reviewing and Editing, Supervision.

Declaration of competing interest

The authors declare that there are no conflicts of interest.

Acknowledgments

References

[1] R. Siegel, C. Desantis, A. Jemal, Colorectal cancer statistics, 2014, CA Cancer J. Clin. 64 (2014) 104—117.

[2] Cancer Today, International Agency for Research on Cancer. https://gco.iarc.fr/ (Accesseed 15 April 2021).

[3] A.J. Breugom, M. Swets, J.F. Bosset, et al., Adjuvant chemotherapy after pre-operative (chemo) radiotherapy and surgery for patients with rectal cancer: a systematic review and meta-analysis of individual patient data, Lancet Oncol. 16 (2015) 200—207.

[4] E. Rajesh, L.S. Sankari, L. Malathi, et al., Naturally occurring products in cancer therapy, J. Pharm. Bioallied Sci. 7 (2015) S181—S183.

[5] U. Rinner, C. Lentsch, C. Aichinger, Syntheses of galbulimima alkaloids, Synthesis 22 (2010) 3763—3784.

[6] P. Lan, A.J. Herlt, A.C. Willis, et al., Structures of new alkaloids from rain forest trees Galbulimima belgraveana and Galbulimima baccata in Papua New Guinea, Indonesia, and northern Australia, ACS Omega 3 (2018) 1912—1921.

[7] B. Thomas, Psychoactive properties of Galbulimima bark, J. Psychoactive Drugs 37 (2005) 109—111.

[8] M. Takadoi, K. Yamaguchi, S. Terashima, Synthetic studies on himbacine, a potent antagonist of the muscarinic M2 subtype receptor. Part 2: synthesis and muscarinic M2 subtype antagonistic activity of the novel himbacine congeners modified at the C-3 position of lactone moiety, Bioorg. Med. Chem. 11 (2003) 1169—1186.

[9] M.M. Young, M. Kester, H.G. Wang, Sphingolipids: regulators of crosstalk between apoptosis and autophagy, J. Lipid Res. 54 (2013) 5—19.

[10] B.E. Fitzwalter, A. Thorburn, Recent insights into cell death and autophagy, FEBS J. 282 (2015) 4279—4288.

[11] S. Deng, M.K. Shanmugam, A.P. Kumar, et al., Targeting autophagy using natural compounds for cancer prevention and therapy, Cancer 125 (2019) 1228—1246.

[12] L. Yuan, S. Wei, J. Wang, et al., Isoorientin induces apoptosis and autophagy simultaneously by reactive oxygen species (ROS)-related p53, PI3K/Akt, JNK, and p38 signaling pathways in HepG2 cancer cells, J. Agric. Food Chem. 62 (2014) 5390—5400.

[13] J.J. Bravo-Cordero, L. Hodgson, J. Condeelis, Directed cell invasion and migration during metastasis, Curr. Opin. Cell Biol. 24 (2012) 277—283.

[14] C.L. Chaffer, R.A. Weinberg, A perspective on cancer cell metastasis, Science 331 (2011) 1559—1564.

[15] X.D. Xu, S.X. Shao, H.P. Jiang, et al., Warburg effect or reverse Warburg effect? A review of cancer metabolism, Oncol. Res. Treat. 38 (2015) 117—122.

[16] O. Warburg, F. Wind, E. Negelein, The metabolism of tumors in the body, J. Gen. Physiol. 8 (1927) 519—530.

[17] L. Bai, S. Wang, Targeting apoptosis pathways for new cancer therapeutics, Annu. Rev. Med. 65 (2014) 139—155.

[18] C. Bonvin, A. Guillon, M.X. van Bemmelen, et al., Role of the amino-terminal domains of MEKKs in the activation of NF kappa B and MAPK pathways and in the regulation of cell proliferation and apoptosis, Cell. Signal. 14 (2002) 123—131.

[19] M. Stankiewicz, W. Jonas, E. Hadas, et al., Supravital staining of eosinophils, Int. J. Parasitol. 26 (1996) 445—446.

[20] A. Biederbick, H.F. Kern, H.P. Elsässer, Monodansylcadaverine (MDC) is a specific in vivo marker for autophagic vacuoles, Eur. J. Cell Biol. 66 (1995) 3—14.

[21] Y. Kabeya, N. Mizushima, A. Yamamoto, et al., LC3, GABARAP and GATE16 localize to autophagosomal membrane depending on form-II formation, J. Cell Sci. 117 (2004) 2805—2812.

[22] Y. Kabeya, N. Mizushima, T. Ueno, et al., LC3, a mammalian homologue of yeast Apg8p, is localized in autophagosome membranes after processing, EMBO J. 19 (2000) 5720—5728.

[23] J. Kim, M. Kundu, B. Viollet, et al., AMPK and mTOR regulate autophagy through direct phosphorylation of Ulk1, Nat. Cell Biol. 13 (2011) 132—141.

[24] P. Vihinen, R. Ala-aho, V.M. Kähäri, Matrix metalloproteinases as therapeutic targets in cancer, Curr. Cancer Drug Targets 5 (2005) 203—220.

[25] C.J. Lee, M.H. Lee, S.M. Yoo, et al., Magnolin inhibits cell migration and invasion by targeting the ERKs/RSK2 signaling pathway, BMC Cancer 15 (2015) 576.

[26] A. Abe, H. Yamada, S. Moriya, et al., The β-carboline alkaloid harmol induces cell death via autophagy but not apoptosis in human non-small cell lung cancer A549 cells, Biol. Pharm. Bull. 34 (2011) 1264—1272.

[27] S. Bialik, S.K. Dasari, A. Kimchi, Autophagy-dependent cell death - where, how and why a cell eats itself to death, J. Cell Sci. 131 (2018), jcs215152.

[28] D. Denton, S. Kumar, Autophagy-dependent cell death, Cell Death Differ. 26 (2019) 605—616.

[29] M. Zhang, L. Su, Z. Xiao, et al., Methyl jasmonate induces apoptosis and pro-apoptotic autophagy via the ROS pathway in human non-small cell lung cancer, Am. J. Cancer Res. 6 (2016) 187—199.

[30] B.Y. Law, S.W. Mok, W.K. Chan, et al., Hernandezine, a novel AMPK activator induces autophagic cell death in drug-resistant cancers, Oncotarget 7 (2016) 8090—8104.

[31] P.J. Roach, AMPK -> ULK1 -> autophagy, Mol. Cell Biol. 31 (2011) 3082—3084.

[32] E.K. Yoon, Y.T. Jeong, X. Li, et al., Glyceollin improves endoplasmic reticulum stress-induced insulin resistance through CaMKK-AMPK pathway in L6 myotubes, J. Nutr. Biochem. 24 (2013) 1053—1061.

[33] X. Fan, J. Wang, J. Hou, et al., Berberine alleviates ox-LDL induced inflammatory factors by up-regulation of autophagy via AMPK/mTOR signaling pathway, J. Transl. Med. 13 (2015), 92.

[34] H.P. Kuo, T.C. Chuang, S.C. Tsai, et al., Berberine, an isoquinoline alkaloid, inhibits the metastatic potential of breast cancer cells via Akt pathway modulation, J. Agric. Food Chem. 60 (2012) 9649—9658.

[35] M. Paauwe, M. Schoonderwoerd, R. Helderman, et al., Endoglin expression on cancer-associated fibroblasts regulates invasion and stimulates colorectal cancer metastasis, Clin. Cancer Res. 24 (2018) 6331—6344.

[36] M. Stankic, S. Pavlovic, Y. Chin, et al., TGF-β-Id1 signaling opposes Twist1 and promotes metastatic colonization via a mesenchymal-to-epithelial transition, Cell Rep. 5 (2013) 1228—1242.

[37] Y. Yun, R. Gao, H. Yue, et al., Sulfate aerosols promote lung cancer metastasis by epigenetically regulating the epithelial-to-mesenchymal transition (EMT), Environ. Sci. Technol. 51 (2017) 11401—11411.

[38] R.J. Araújo Jr, G.A. Lira, J.A. Vilaça, et al., Prognostic and diagnostic implications of MMP-2, MMP-9, and VEGF-α expressions in colorectal cancer, Pathol. Res. Pract. 211 (2015) 71—77.

[39] D.C. Wallace, Mitochondria and cancer, Nat. Rev. Cancer 12 (2012) 685—698.

[40] S.P. Desai, S.N. Bhatia, M. Toner, et al., Mitochondrial localization and the persistent migration of epithelial cancer cells, Biophys. J. 104 (2013) 2077—2088.

[41] P.E. Porporato, V.L. Payen, J. Pérez-Escuredo, et al., A mitochondrial switch promotes tumor metastasis, Cell Rep. 8 (2014) 754—766.

[42] M. López-Lázaro, Digitoxin as an anticancer agent with selectivity for cancer cells: possible mechanisms involved, Expert Opin. Ther. Targets 11 (2007) 1043—1053.

[43] T.L. Serafim, J.A. Matos, V.A. Sardão, et al., Sanguinarine cytotoxicity on mouse melanoma K1735-M2 cells–nuclear vs. mitochondrial effects, Biochem. Pharmacol. 76 (2008) 1459—1475.

[44] V. Estrella, T. Chen, M. Lloyd, et al., Acidity generated by the tumor microenvironment drives local invasion, Cancer Res. 73 (2013) 1524—1535.